Journal of International Conference Series, *1(4):212-228*
ISSN: 5280-7221. August, 2020

http://accexgate.com | vconference@accexgate.com

MODELING AND SIMULATION OF SOLAR ABSORPTION COOLING SYSTEM FOR MAIDUGURI BORNO STATE NIGERIA

Engr. Mai Bukar Ngawaitu
Department of Mechanical Engineering, Ramat Polytechnic Maiduguri Nigeria | Email: nmaibukar@gmail.com

Abdullahi Madu
Federal College of Education (Technical) Potiskum, Yobe State Nigeria | Email: alaminabdallah06@gmail.com

ABSTRACT

The use of solar energy for cooling purposes is an attractive prospect; the key factor for this application is the availability of solar energy for Maiduguri climate and suitable cooling technology. The study aimed to model and simulate solar absorption cooling system for Maiduguri, in order to develop a model for vapor absorption cooling system, evaluate the coefficient of performance (COP) of the vapor absorption cooling system, and optimize the coefficient of performance (COP) .and validation studies of the COP. Aspen plus was used to simulate the solar-powered lithium bromide absorption system. The generator and absorber were modeled by using a multipurpose flash column. ASPEN PLUS uses the flash column to visualize generator and absorber operations. Simultaneously, a modular mode was used to solve the algebraic equations of the flow sheet. The Non-random two-liquid (NRTL) model and latent-heat enthalpy model were used in the simulation to obtain the thermodynamic properties and phase equilibrium of the Lithium bromide solution. The NRTL model software keeps all flashes as three-phase flashes (LLV) or two-phase flashes (LV). Liquid phase activity coefficients are calculated by the NRTL equation by the known values of the liquid phase mass fraction. The NRTL equation is a good method to solve the binary mixture where equilibrium prevails between liquid and vapor. It was discovered that the input values obtained from the optimization (the final values) were different from those of the steady-state simulation carried out prior to the optimization (initial values), also noticed that the final values were within the ranges specified for the input variables during the optimization. The study also noticed that the cooling capacity was increased from 32.3 kW to 430.7 kW while COP increased from 0.684 to 0.793 after optimization.

Keywords*: Cooling, Modeling, Simulation, Solar and Absorption*

BACKGROUND OF THE STUDY

The energy needed to process and circulate air in residential buildings and offices to control humidity, temperature, and cleanliness has increased significantly during the last decade especially in developing countries. High consumption of electricity presents economic and social problems in hot places, caused by the massive use of cooling machines. However, prolonged used of chlorofluocarbon (CFC) and hydrochlorofluocarbon (HCFC) refrigerants cause destruction of the ozone layer, and possible global warming due to excessive burning of fossil fuel. Absorption cooling

system is a more preferable option for energy generation. In absorption cooling system, physiochemical process replaces the mechanical process of the vapor compression system by using energy in the form of heat rather than mechanical work. The absorption refrigerants lithium bromide- water cycle has some attractive features when compared to the conventional cycle. In 2013, Agrouaza *et al* (2017) studied the global modeling of an absorption system working with LiBr/H2O assisted by solar energy. It satisfies the air-conditioning necessities of a classroom in an educational center in Puerto Lumbreras, Murcia, Spain. The absorption system uses a set of solar collectors to satisfy the thermal necessities of the vapor generator. A dynamic simulation model, for a solar powered absorption cooling system was developed, and validated using measured data. Yeung et al (1992) designed and installed a solar driven absorption chiller at the University of Hong Kong; this system included 4.7 kW absorption chillers, flat plate solar collectors with a total area of 38.2 m², water storage tank and the rest of the equipment. They reported that the collector efficiency was estimated at 37.5%, the annual system efficiency at 7.8% and an average solar fraction of 55%, respectively.

The first and most crucial step in the modeling process was finding a suitable property method for the water/lithium bromide mixture. At this point it should be pointed out that except for very common fluids, ASPEN does not use look-up tables for property data. Instead, the user must select a property method based on operating conditions, fluid characteristics, etc. As a result, there is an error inherent to any model created in ASPEN. This should not be taken as a deterrent, as even look-up tables will have some errors due to interpolation. Rather, it is a warning to the potential user to select the property method wisely when modeling in ASPEN. The ASPEN developers suggested that the ELECNRTL property method to be chosen for the water/lithium bromide solution based on the operating conditions and fluids being modeled. As the name suggests, it is a method designed for electrolytes. To use it properly, the user must select the relevant components (in this case, water and lithium bromide) and use the electrolyte wizard, which will generate a series of reactions. In this case, the only relevant reaction was the dissociation of lithium bromide. For the states that are pure water, the steams were used (Herold *et al*, 1996). Since look-up tables are available for pure steam, the property data induced error will be much smaller.

METHODOLOGY

Materials

Aspen Plus V8.4 Software was used for the modeling and simulation of the Solar absorption cooling system. The inputs to the Model were mainly data collected from Borno state meteorological Agency for the year 2016.

METHODS

The theory of absorption refrigeration system working with Lithium Bromide (LiBr) and water, illustrated by Figure 1, consist of a condenser, an expansion valve, an evaporator and a thermal compressor. In this cycle, water condenses (rejecting heat) and evaporates (extracting heat from the thermal load) similar to a refrigeration cycle by mechanical compression. However, the thermal compressor located between the evaporator and condenser, performs vapor compressor by using energy in the form of heat (solar energy in this case).

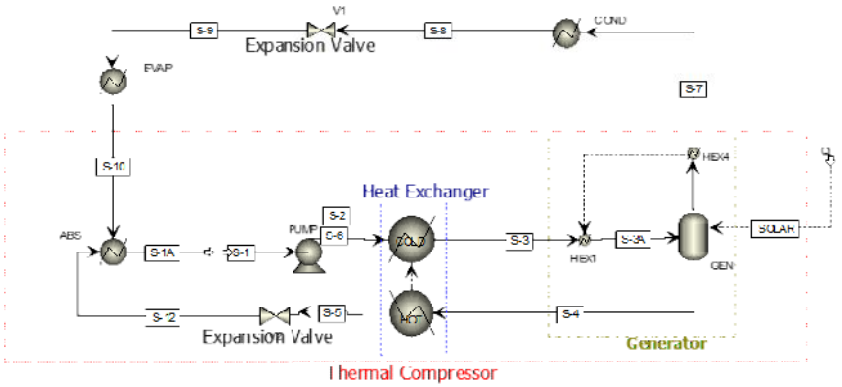

Figure 1: Process Diagram of the Water-LiBr absorption refrigerator

PROCESS DESCRIPTION

The thermal compressor consists of two major unit operations: Absorption and distillation. In the absorption water vapor is absorbed by LiBr due to it affinity with water forming a weak LiBr/water solution in the absorber and in distillation (generator) the water vapor is separated from the strong LiBr/Water solution consuming heat. For a better cycle efficiency, separation must be almost complete, and water quality must be close to 1 (~0.999) in the generator output (Herold, et al., 1996). For improvement of the efficiency of the system, a regenerative heat exchanger is used between the absorber and generator. Generally, the heat is removed from the system by cooling tower. The cooling water passes through the absorber first then the condenser. The temperature of the absorber has a higher influence on the system efficiency than the condensing temperature of the cooling tower where the heat is dissipated to the environment. In the case that the sun is not shining, an auxiliary heat source is used by electricity or conventional boiler to heat the water to the required generator temperature. It is highly recommended to use a partitioned hot-water storage tank to serve as two separate tanks. In the morning, the collector system is connected to the upper part of the tank, whereas in the afternoon, the whole tank would be used to provide heat energy to the system.

Electrical energy consumption in an absorption cycle is minimal when compared to a compression cycle, since only the pump uses this energy to raise the pressure of the liquid solution formed in the absorber. In a vapor compression cycle, the compressor consumes much more electrical energy to raise the pressure of the refrigerant vapor that comes out of the evaporator. Table 1 describes the block used in ASPEN PLUS to represent each unit operation in the process.

Table 1: ASPEN PLUS Model Representation adopted from Balghouthi et al, 2008.

Units	Block	Descriptions
Cond	Heater (Exchanger)	Condenser
V1 and V2	Valve	Expansion Valve 1 and 2
Evap	Heater (Exchanger)	Evaporator
ABS	Heater (Exchanger)	Absorber
PUMP	Pump	Pump
Heat Exchanger	Heater (Exchanger)	Regenerative Heat Exchanger
GEN	Flash2	Distillation
Hex1	Heater (Exchanger)	vapor heat control
Hex4	Heater (Exchanger)	vapor heat control

Table 2. below shows average solar radiation collected from Borno state meteorological Agency for the year 2017.

Month	**T.max**	**T. min**	**T.mean**	**R.H**	**Evaporation**	**Sunshine**
No	0C	0C	0C	%	Mm	0C
January	31.6	0.9	26.1	19	10.8	9.0
February	33.0	14.5	28.7	16	13.7	9.1
March	38.5	18.8	29.3	12	16.8	9.6
April	41.1	25.3	33.3	26	15.9	9.0
May	40.2	26.7	31.0	39	13.4	9.1
June	36.0	24.7	29.1	57	3.8	6.5
July	33.0	23.6	27.4	67	5.5	7.2
August	30.9	22.6	27.2	75	2.9	6.6
September	33.3	22.5	27.2	69	3.7	7.9
October	35.3	19.9	28.5	43	7.6	7.2
November	35.2	14.8	27.6	26	9.7	7.9
December	35.7	12.9	26.2	25	9.5	7.8

T. max = Temperature maximum
T. min = Temperature minimum
T. Mean = Average
R H = Relative Humidity

SYSTEM DESCRIPTION

The solar-powered absorption cycle consists of four major parts, i.e., a generator, a condenser, an evaporator and an absorber. These major components are divided into three parts by one heat exchanger, two expansion valves and a pump. Schematic diagrams of the solar-powered cooling system are shown in Figures 2 and 3. Initially, the collector receives energy from sunlight and heat is accumulated in the storage tank.Subsequently, the energy is transferred through the high temperature energy storage tank to the refrigeration system. The solar collector heat is used to separate the water vapor, stream number 2, from the lithium bromide solution, stream number 3,

in the generator at high temperature and pressure resulting in higher lithium bromide solution concentration. Then, the water vapor passes to the condenser where heat is removed and the vapor cools down to form a liquid, stream number 4. The liquid water at high pressure, stream number 4, is passed through the expansion valve, stream number 9, to the evaporator, where it gets evaporated at low pressure, thereby providing cooling to the space to be cooled. The weak solution, stream number8, is then pumped into the generator and the process is repeated.

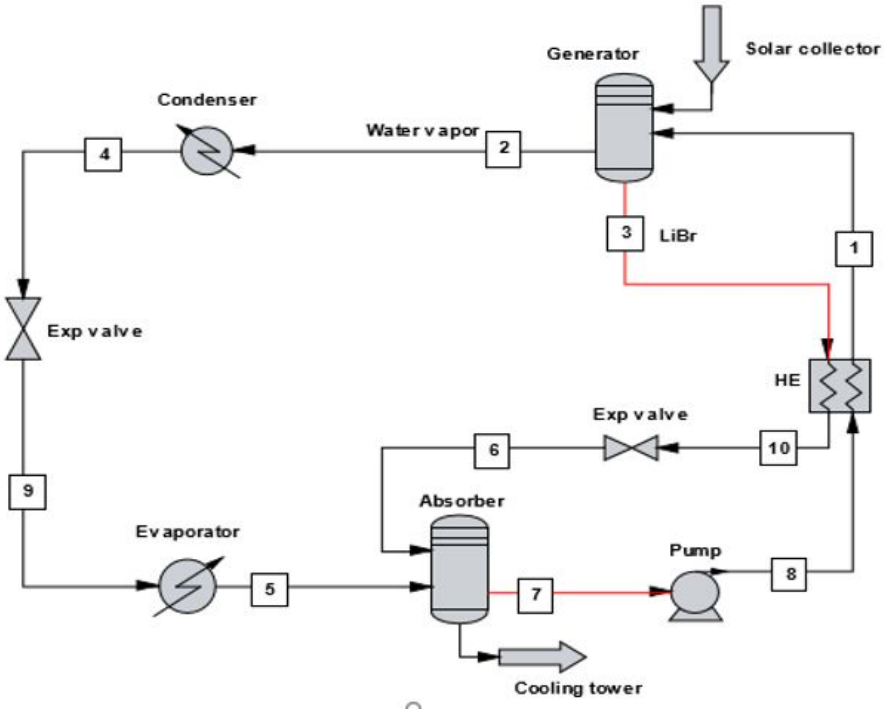

Figure 2: Schematic diagram of the absorption cycle adopted from Balghouthi, et al 2008.

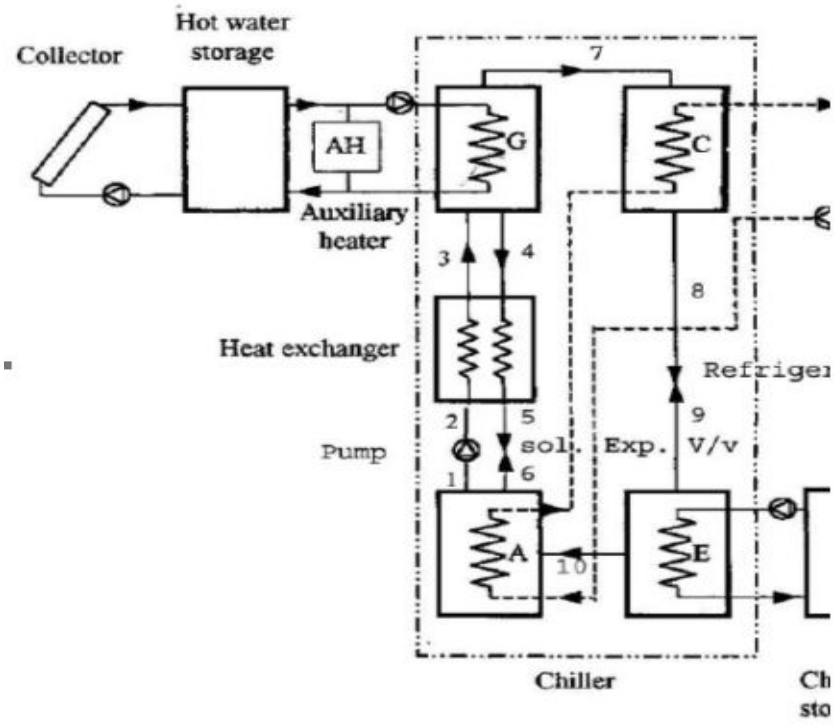

Figure 3 Schematic Diagram of the solar-powered cooling system adopted from Balghouthi, et al 2008. A-Absorber, G- generator, C- Condenser, E- Evaporator

Generally, the heat is removed from the system by a cooling tower. The cooling water passes through the absorber first then the condenser. The temperature of the absorber has a higher influence on the system efficiency than the condensing temperature of the cooling tower where the heat is dissipated to the environment. In the case that the sun is not shining, an auxiliary heat source is used by electricity or conventional boiler to heat the water to the required generator temperature.

MATHEMATICAL MODEL

Preliminary material balance is taken across each unit i.e. the generator, absorber, evaporator, condenser and heat exchanger to analyze the working conditions of all components of the system. Energy balances are performed and a computer simulation is developed for the cycle analysis. A control volume analysis around each component, which covered the rate of heat addition in the generator, and the energy input of the cycle, is given by equation Klein, (2018). (3.1):

$$Q_{Generator} = Q_{Solar} = m_4 h_4 + m_7 h_7 - m_3 h_3 \quad (3.1)$$

The rate of heat rejection out of the condenser is given equation (3.2):

$$Q_{Cond} = m_7 (h_7 - h_8) \quad (3.2)$$

The rate of heat absorption of the evaporator is given by equation (3.3):

$$Q_{Evap} = m_9(h_{10} - h_9) \quad (3.3)$$

The rate of heat rejection of the absorber is given by equation (3.4):

$$Q_{AES} = m_{10}h_{10} + m_{12}h_{12} - m_1h_1 \quad (3.4)$$

An energy balance on the hot side of the heat exchanger is given by equation (3.5):

$$Q_{shx-hot} = m_4(h_4 - h_5) \quad (3.5)$$

Similarly, an energy balance on the cold side of the heat exchanger is given by equation (3.6):

$$Q_{shx-cold} = m_2(h_3 - h_2) \quad (3.6)$$

Coefficient of performance (COP) according to Figure 3.1. is defined as follows:

$$COP = \frac{Q_{Evap}}{Q_{Generator} + Q_{Pump}} \quad (3.7)$$

The solar collector was modeled in this manner proposed by Klein.(2018). The basic equation for the rate of useful energy gain by a flat-plate solar collector is given by:

$$Q_S = F_r A_C(IR - U_L(T_{ci} - T_a) \quad (3.8)$$

Where:

F_r = collector heat removal factor (0.8)

I = radiation intensity, W/m^{2}K

R = ratio of total radiation on tilted surface to that on plane of measurement (1.08)

U_L = overall loss heat transfer coefficient, W/m2oK, (7.811)

T_c = temperature of the Collector surface (48^{o}C)

T_a = ambient temperature (25^{o}C)

For simplicity, the above values in bracket will be use based on the results obtained by Dara, (2010).Radiation Intensity (I)was obtained from monthly daily average solar energy parameters measured in Maiduguri by (Luqman, et al., 2016).

SETTING UP ASPEN PLUS V8.4

The first step was to add the components of interest, in this case water, lithium bromide as well as the lithium ion Li+ and the bromide ion Br- as seen in Figure 3.1. Then the electrolyte wizard was used in order to add the chemistry and specify the property method.

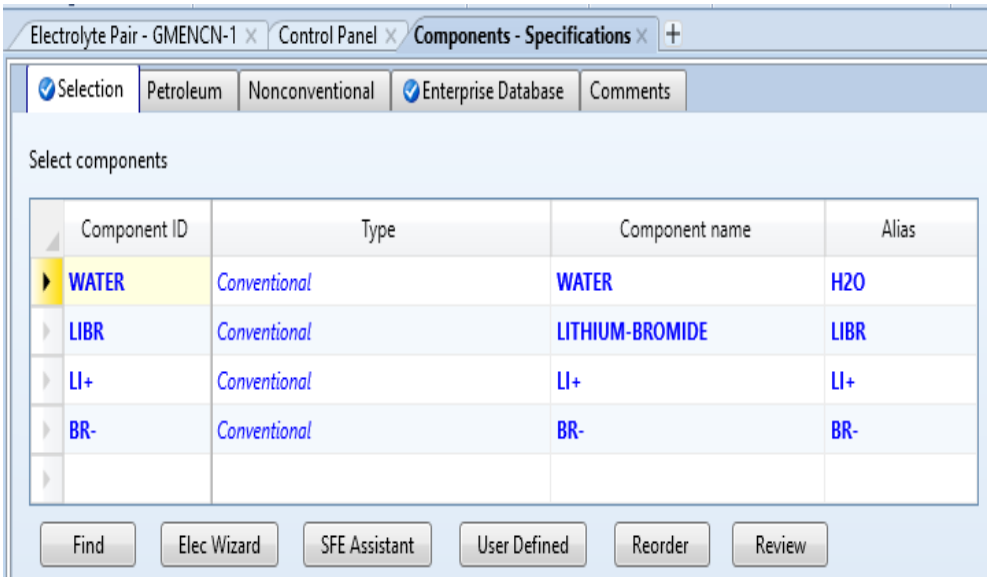

Figure 3: Component specifications required for the absorption cooling system.

The base method of ENRTL-RK, anunsymmetric model, was automatically chosen for the thermodynamics fluid properties base on the chemistry produce by the electrolyte wizard. Once the required components are added the missing data for the components of interest need to be pulled from various Aspen databases. This can be done by clicking on retrieve parameters under the tools heading in the home ribbon. In the case of some electrolytes, in this case lithium bromide, the Aspen database does not contain all of the necessary properties to perform the simulation using Redlich-Kwong as the EOS therefore they must be added in manually. The missing parameters are the critical pressure Pc, critical temperature Tc, critical volume VcandZc of the LiBr. These four values were obtained from the literature (Wikipedia, 2018) as 50, 1726.85, 100 and 0.2 for Pc, Tc, Vc and Zc respectively. These values were entered in the LiBr property column using the review button of Figure 2.

MODEL SIMULATION

Aspen plus was used to simulate the solar-powered lithium bromide absorption system. The generator and absorber were modeled by using a multipurpose flash column. ASPEN PLUS uses the flash column to visualize generator and absorber operations. Simultaneously, a modular mode was used to solve the algebraic equations of the flow sheet. The Non-random two-liquid (NRTL) model and latent-heat enthalpy model were used in the simulation to obtain the thermodynamic properties and phase equilibrium of the Lithium bromide solution. The NRTL model software keeps all flashes as three-phase flashes (LLV) or two-phase flashes (LV). Liquid phase activity coefficients are calculated by the NRTL equation by the known values of the liquid phase mass fraction. The NRTL equation is a good method to solve the binary mixture where equilibrium prevails between liquid and vapor. Previous studies have shown that the NRTL equation is in good agreement with the experimental phase equilibrium of Lithium Bromide solution. The numerical data obtained are in good agreement with Balghouthi et al. (2008) results adopted.

The input data required for simulating the system consists of the following: generator temperature, absorber temperature, generator and condenser pressure, evaporator and absorber pressure, pump output pressure, mass flow rate entering generator, lithium bromide solution concentration entering the generator and fixed saturated liquid state from heat exchanger to generator. Figure 3 shows flow-diagram for how simulation works using input data. The output includes the generator heat gain, cooling capacity and COP.

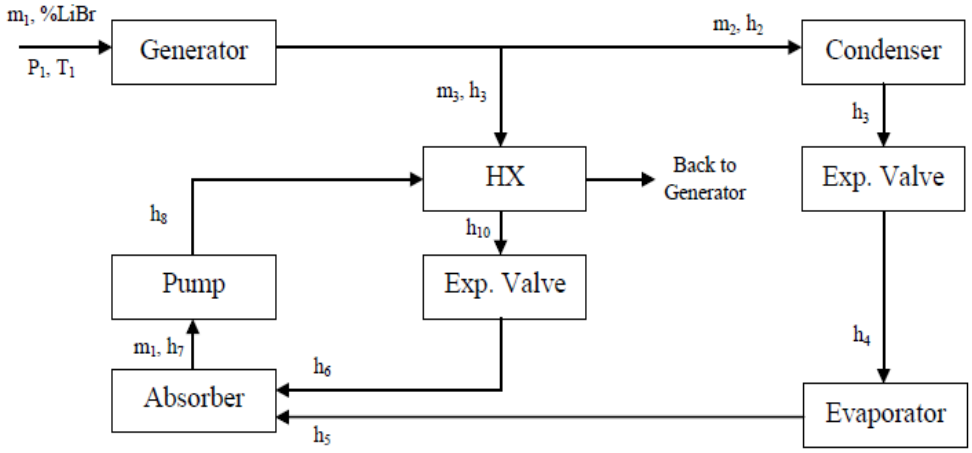

Figure 4: Modified Information-flow diagram for solar-powered absorption cooling system

RESULTS AND DISCUSSIONS

VARIATION OF GENERATOR TEMPERATURE AGAINST COP

The effect of the variation of the generator temperature with Coefficient of performance (COP) and cooling capacity against generator temperature is shown in figure 4.1. The cooling capacity increases rapidly from a low value of 13 kW (at 79^{o}C) up to 669 kW (at 150^{o}C). The COP rises from a low value of 0.24 (at 79^{o}C) to reach a constant value of 0.781 (at 111^{o}C). The cooling capacity increases as the generator temperature increases.

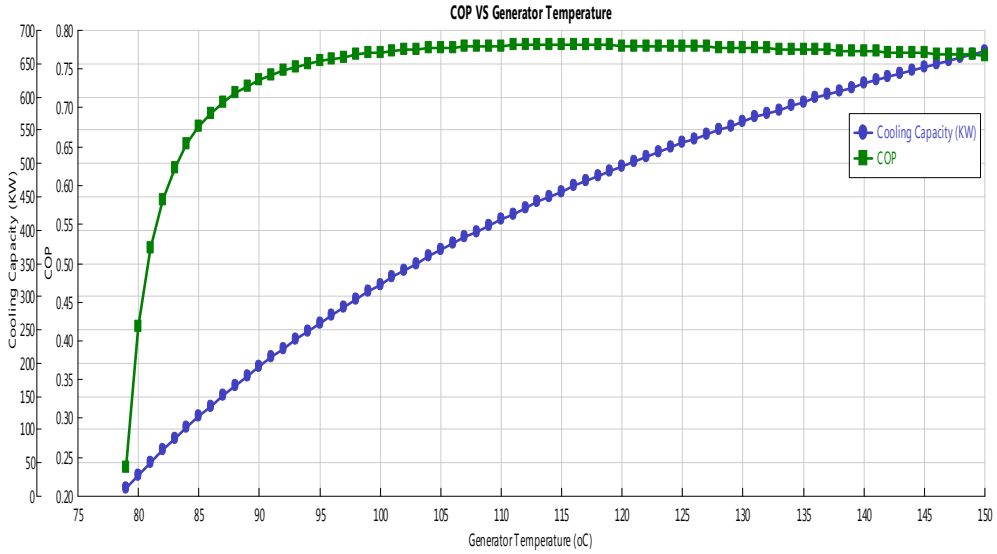

Figure 4: Effect of generator temperature on cooling capacity and COP as Predicted by ASPEN model.

The COP increase significantly with increasing generator/collector temperature, but as the generator/ collector temperature increases, the heat transfer in all the heat exchangers of the system also increases as shown in Figure 4.2. The figure shows similar increase in the heat transfer in all of evaporator, condenser and absorber when varying the generator (or collector) temperature.The concentration of Lithium Bromide (LiBr) solution increases rapidly with increase in generator temperature (See Figure 6). This is expected, since more water evaporate with temperature which result in more LiBr with less water in the generator (hence higher concentration).

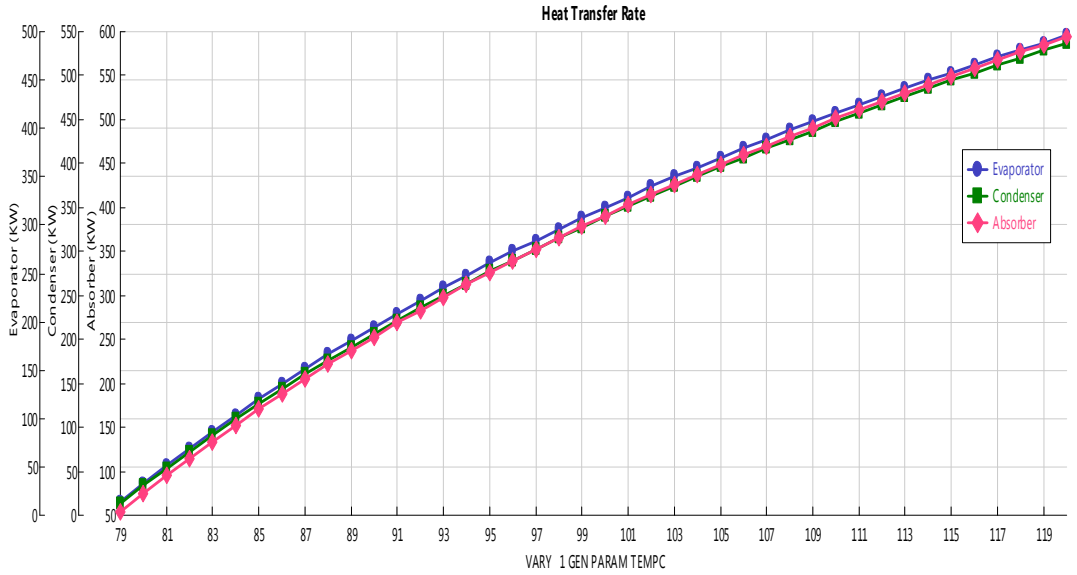

Figure 5: Effect of generator inlet temperature on evaporator, absorber, condenser against generator heat transfer rates.

The concentration of Lithium Bromide (LiBr) solution increases rapidly with increase in generator temperature (See Figure 6). This is expected since more water evaporates with temperatures which result in more LiBr with less water in the generator (hence higher concentration).

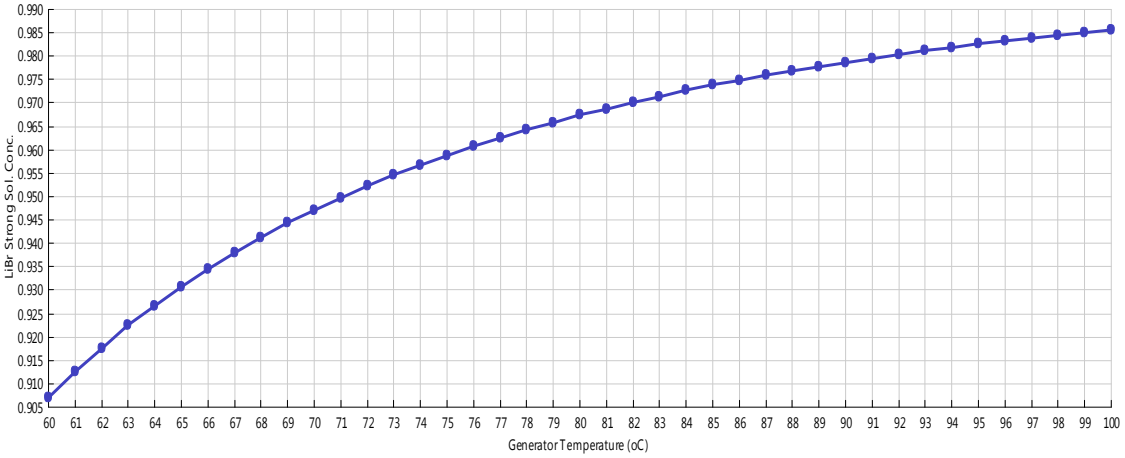

Figure 6: Effect of generator temperature (^0C) on LiBr-H_2O concentration (kg)

The generator inlet temperature could not be increased or decreased too much because of the crystallization of the lithium bromide as seen in figure 4.4. Because lithium bromide is a salt, in its solid state it has a crystalline structure. There is a specific minimum solution temperature for any given salt concentration when lithium bromide is dissolved in water. The salt begins to leave the solution and crystallize below this minimum temperature. In an absorption system, if the LiBr-solution concentration is too high or if the LiBr-solution temperature is reduced too low, crystallization may occur. The crystallization influences the cycle performance and the temperatures at different streams.

There are several causes for crystallization. Air leakage into the system is one of most common reason for crystallization. Air leakage results in increased pressure in the evaporator. This, in turn, results in higher evaporator temperatures and, consequently, lower cooling capacities. In the other case, at high load conditions, the control system increases the heat input to the generator, resulting in increased solution concentrations to the level where crystallization may occur. Non-absorbable gases, like hydrogen, produced during corrosion, can also be present; this can reduce the performance of both the condenser and the absorber. Electric power failure is found to be another reason for crystallization. Crystallization is most likely to occur when the machine is stopped while operating at full load, when highly concentrated solutions are present in the solution heat exchanger. To solve this problem, during normal shutdown, the system should go into a dilution cycle, which lowers the concentration of the LiBr-solution throughout the system, so that the machine may cool to ambient temperature without crystallization occurring in the solutions.

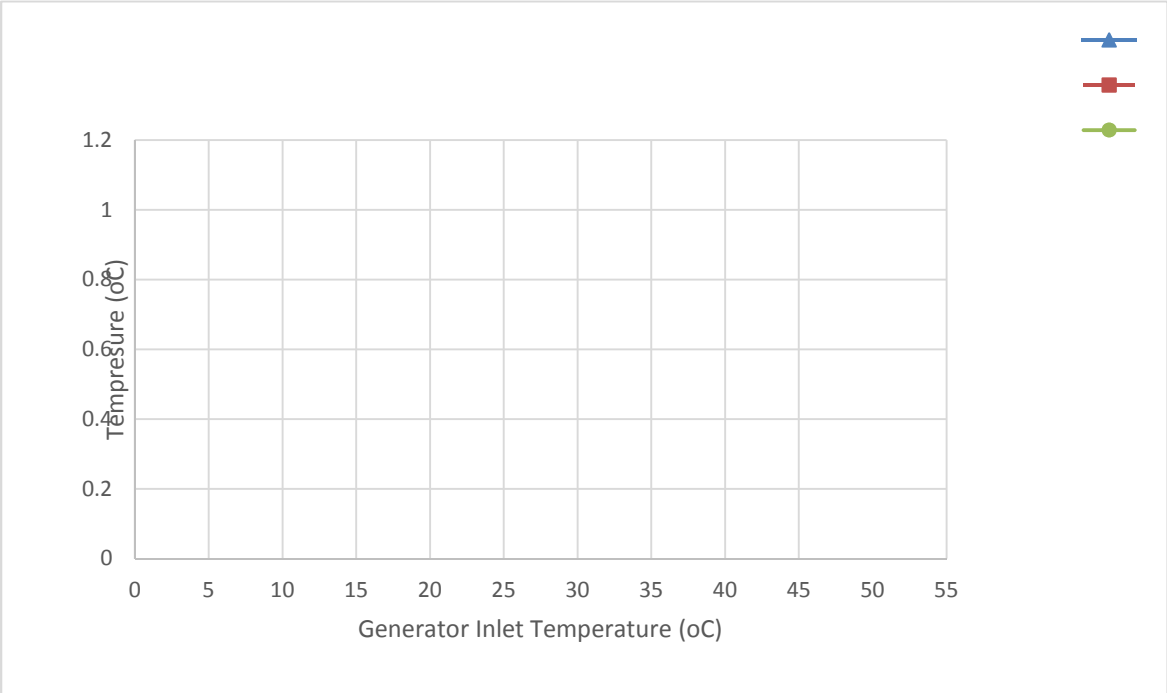

Figure 7: Effect of generator inlet temperature on generator, evaporator and condenser temperatures.

VARIATION OF EVAPORATOR TEMPERATURE AGAINST COP

The greater the collector area the greater the heat gained. This can be good for the auxiliary boiler as seen in figure 7 above. Once the heat gained is increased, less heat is required from the auxiliary boiler to maintain the required generator temperature. The next parameter of interest is evaporator temperature. This is an important parameter to consider because it has a significant effect on chiller performance, as a higher evaporator temperature means a higher COP. The evaporator temperature is a set value that is dictated by the desired cooling temperature, but since a variety of cooling temperatures are needed in an LNG plant, it is important to consider a variety of evaporator temperatures.

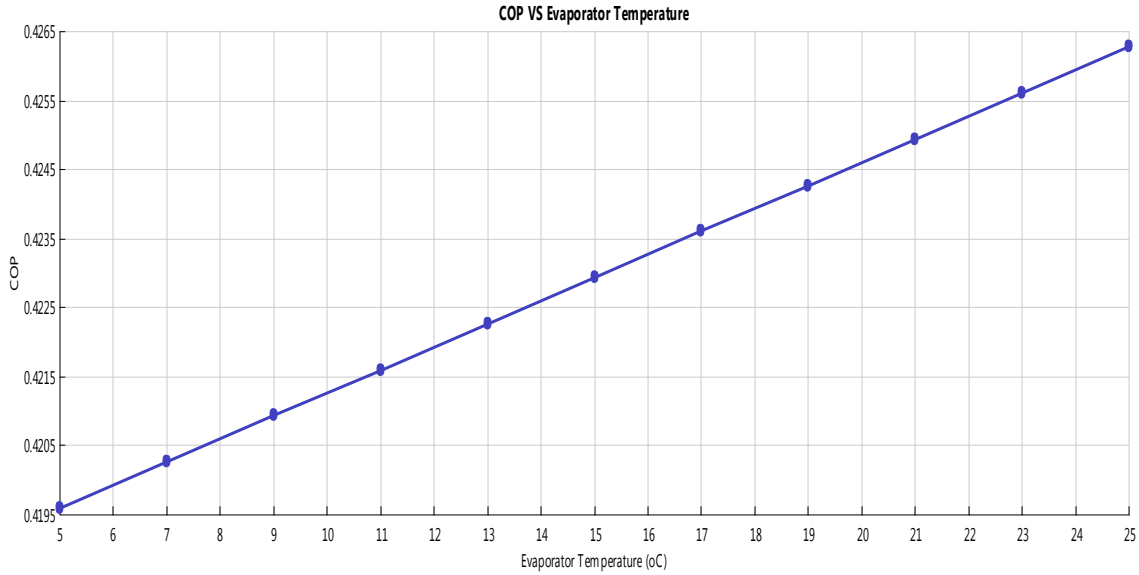

Figure 8: Effect of evaporator temperature on absorption cooling system COP as predicted by ASPEN model

From this Figure, it can be seen that; within the range of temperature investigated, the absorption cooling system COP Increases from 0.4195 to 0.4262.

VARIATION OF LITHIUM BROMIDE CONCENTRATION AGAINST COP

In this section, Lithium Bromide concentration was varied in the refrigerate solution in other to determine it significant on the COP. From Figure 9, it is shown that the COP decreases rapidly with increase in LiBr-concentration. From this Figure, an increase in the concentration of LiBr from 0.03 to 0.88 LiBr kg/kg solution resulted in a decrease in the COP from 37 to 2 %. This is due to the little or lack of the absorbent (water) present for circulation in higher concentration of LiBr. Since higher LiBr concentration, means lower water present.

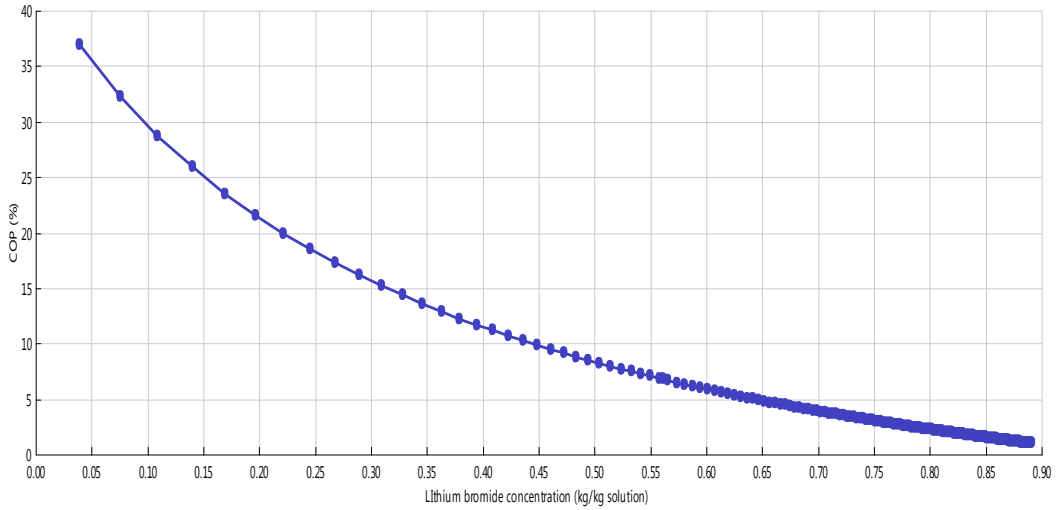

Figure 9: Effect of lithium-bromide concentration on the COP as predicted by Aspen model.

VARIATION OF SOLAR COLLECTOR AREA AGAINST COP

Increase in solar collector area on the same setting will supply more energy to the system, which in turn increase the temperature of the generator thereby making more water to evaporate, this decrease the performance of the system. This behavior is depicted in Figure 10.

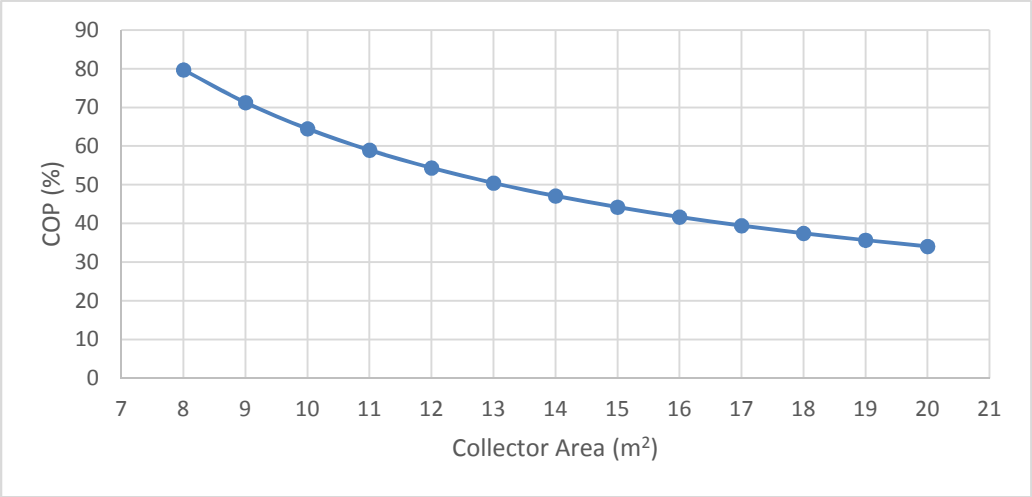

Figure 10: Effect of Solar Collector area on the COP as predicted by Aspen model.

VARIATION OF SOLAR INSOLATION AGAINST MONTHS OF THE YEAR

Figure 11. Illustrate a typical climatic condition of Maiduguri in a particular month, as depicted by the insolation variation in the month. This values used in the model to provide the heat required in the generator based on Equation 3.8. From this Figure, it can be seen that more heat (energy) is expected between Augusts to December of the year.

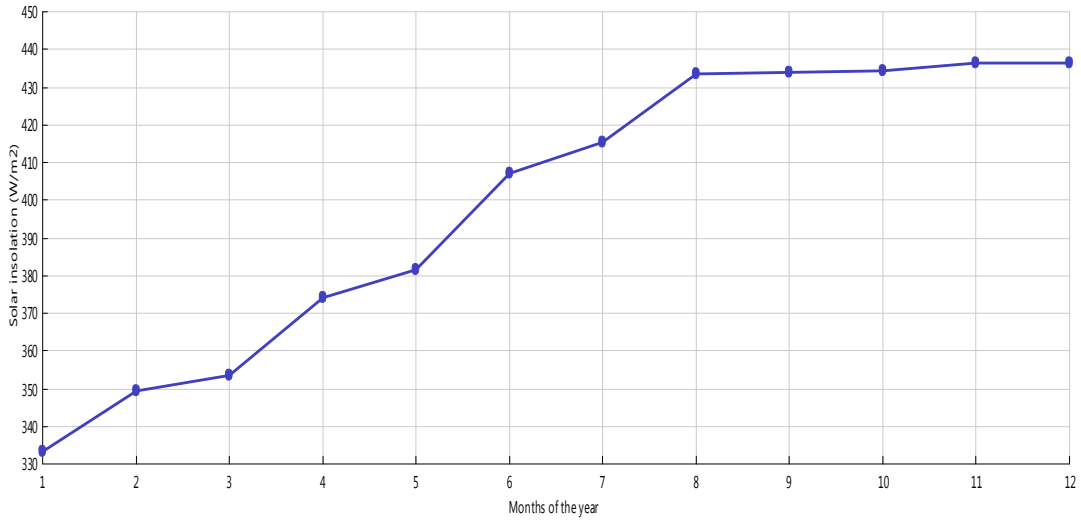

Figure 11: Effect of Solar Collector area on the COP as predicted by Aspen model.

VALIDATION OF THE DEVELOPED MODEL

The operational validation of the developed model in table 4.1 shows comparison between TRNSYS (a) adopted from Balghouthi et al, 2008 and Aspen plus (b)

Table 3: Modified Operational condition (a) (Balghouthi, et al., 2008), adopted and (b) ASPEN PLUS process model.

		T (^{o}C)		P (kPa)		x(kg LiBr/kg solution)		m (kg/s)	
Stream		(a)	(b)	(a)	(b)	(a)	(b)	(a)	(b)
1	Pump Outlet	36.2	8.1	6.601	6.601	0.561	0.561	0.056	0.056
2	Condenser Inlet	70	78	6.601	6.601	0	0	0.0048	0.023419
3	Generator Outlet	84.6	78	6.601	6.601	0.613	0.964	0.0512	0.032581
4	Condenser outlet to exp. Valve	38	37.8	6.601	6.601	0	0	0.0048	0.023419
5	Vapor from evaporator to absorber	4.4	5	0.9	0.9	0	0	0.0048	0.023419
6	Solution inlet in absorber	47.1	39.1	0.9	0.9	0.613	0.964	0.0512	0.023419
7	Absorber outlet	36.2	8.1	0.9	0.9	0.561	0.561	0.056	0.032581
8	Generator inlet from heat exchanger	62.4	62.4	6.601	6.601	0.556	0.561	0.056	0.032581
9	Evaporator inlet from expansion valve	5.5	4.5	0.9	0.9	0	0	0.0048	0.023419
10	Absorber inlet from heat exchanger	53.6	53.6	6.601	6.601	0.613	0.964	0.0512	0.032581
11	Absorber inlet from exp. Valve	62.4	39.1	0.9	0.9	0.556	0.964	0.056	0.032581

OPTIMIZATION PROCESS

As can be observed from the above analyses based on the input variables (generator temperature and evaporator temperature), the tangible input value(s) that will give highest COP and high cooling capacity has not been obtained. This called for the optimization of the process using the same Aspen Plus model. The optimization of this process was carried out to obtain the optimum input variables that would give the maximum COP and Cooling Capacity on bi-objective function using equation 4.1, where α varied from 0 to 1. The input variables were varied based on the knowledge gained from the parametric analysis (see second column in Table 4.2) and COP_{max} was set as the objectives function. The optimum input variables obtained from the optimization carried out and those of the steady-state simulation carried out prior to it (the optimization) are also presented in Table 4.2. From the table, it was discovered that the input values obtained from the optimization (the final values) were different from those of the steady-state simulation carried out prior to the optimization (initial values), also noticed that the final values were within the ranges specified for the input variables during the optimization.

$$COP_{max} = \alpha(COP) + (1 - \alpha)(Cooling\ Capacity) \quad (4.1)$$

Table 4: Initial input (or steady-state) and optimum parameters obtained from the process

Variable	Initial value	Final Value	Units
Generator Temperature	48	110	^{o}C
Evaporator Temperature	5	24	^{o}C

Presented in Table 5 are the initial and final values of the objective function recorded before and after optimization;

Table 5: Objectives Function

Variable	Initial value	Final Value
Cooling Capacity	32.3 kW	430.7 kW
COP	0.684	0.793

From Table 5, it was noticed that the optimized values were different from their steady-state values, just as it was discovered in the case of the steady-state and the optimum input variables. Specifically, the cooling capacity was increase from 32.3 to 430.7 kW while COP increased from 0.684 to 0.793 after optimization.

CONCLUSION

The study developed a model for vapor absorption cooling system and evaluated the coefficient of performance (COP) of the vapor absorption cooling system, optimized the coefficient of performance (COP) .and validation studies of the COP was also conducted. In conclusion, the following were observed:

i. The input values obtained from the optimization (the final values) were different from those of the steady-state simulation carried out prior to the optimization (initial values).
ii. The final values were within the ranges specified for the input variables during the optimization.
iii. The cooling capacity was increased from 32.3 kW to 430.7 kW while COP increased from 0.684 to 0.793 after optimization.

REFERENCES

Agrouaza, Y.; Bouhal, T.; Allouhi, A.; Kousksou, T.; Jamil, A.; Zeraouli, Y. (2017**).** *Energy and parametric analysis of solar absorption cooling systems in various Moroccan climates*. Case Stud. Therm. Eng. 9, 28–39

Balghouthi, M., Chahbani, M. H., & Guizani, A. (2008). Feasibility of solar absorption air conditioning in Tunisia. *Building and environment*, *43*(9), 1459-1470.

Dara, J.E, (2010). *Modeling and evaluation of Paasive Flat- plate solar collector*, AKWA: Nnamdi Azikiwe University.

Herold, K.E., Radermacher, R., and Klein, S, (1996). "Absorption chillers and heat pumps, CRC Press, Boca Raton. *International Journal of Refrigeration*, 24(6): 531-543.

Klein, S.A.(2018) EES Engineering Equation Solver, User Manual, F-Chart Software

Yeung M.R., Yueu P.K., Dunn A., Cornish L.S., (1992). *Performance of a solar powered air conditioning system in Hong Kong, Solar energy*, 48(5): 309-319.